

含时滞的忆阻耦合 HR 神经元的复杂放电行为 *

王松 茅晓晨 †

(河海大学 力学与材料学院,南京 211100)

摘要 本文研究具有忆阻的两耦合 Hindmarsh-Rose 神经元系统,考虑了神经元间信号传输过程中的时滞效应.借助平衡点的稳定性分析,获得与时滞相关的稳定条件.通过数值算例验证理论结果,揭示各类丰富而有趣的动力学现象,如多种簇放电行为等.搭建相应的耦合神经元电路实验平台,取得与理论分析和数值计算相吻合的结果.研究结果表明,时滞是影响系统稳定性和放电模式的重要因素.

关键词 Hindmarsh-Rose 神经元, 时滞, 忆阻, 放电行为, 电路实验

DOI: 10.6052/1672-6553-2020-005

引言

神经元是神经系统基本的结构和功能单元.20世纪 50 年代, Hodgkin 和 Huxley 在研究乌贼神经轴突电生理活动中提出了著名的 Hodgkin-Huxley (H-H) 神经元模型^[1].1961 年, FitzHugh 提出了二维简化模型, 并由 Nagumo 构建了相应的电路.在此基础上, Hindmarsh 和 Rose 提出了具有慢时间尺度的三维系统, 可用于模拟神经元的簇放电特性^[2].随后, 有关 HR 神经元网络动力学研究的报道不断涌现^[3,4,6-8].

由于信号传输速度的有限性和递质释放的滞后, 时滞在神经网络中是难以避免的.已有研究表明, 耦合过程中的时滞会显著影响到系统的稳定性和同步模式等动力学特性^[5-8].Lakshmanan 等人^[6]研究了含时滞的 HR 神经元的稳定性、Hopf 分岔、混沌及其控制, 并给出了非线性反馈控制策略以实现主从 HR 神经元之间的同步. Steur 等人^[7]考察了不同拓扑结构情况下时滞耦合 HR 神经网络的同步和部分同步, 并给出了相应的电路实验结果.

美国惠普公司实验室 Strukov 等人在极小型电路中证实了忆阻的存在^[9].忆阻器是一种有记忆功能的非线性电阻元件^[10], 可用于模拟神经元的突触结构^[11].Zhang 等人^[12]研究了基于忆阻的耦合

FitzHugh-Nagumo 神经元模型, 探讨了初始条件对于混沌振荡以及同步过程的影响机制.Thottil 等人^[13]分析了不同忆阻形式耦合的两 HR 神经元网络, 揭示了同步、振荡死亡、混沌以及“near-death rare spikes”等有趣的动力学行为.

本文研究忆阻型 HR 神经网络的动力学行为.该网络由两个含自连接的 HR 神经元通过双向时滞连接相互耦合而成, 在自连接和互连接上均考虑了忆阻.

1 平衡点的稳定性分析

本文的忆阻器模型如文献[11]所示, 相应的耦合神经元网络可用以下一组时滞微分方程描述:

$$\begin{cases} \dot{x}_{1,2} = y_{1,2} - ax_{1,2}^3 + bx_{1,2}^2 - z_{1,2} + I + \\ \quad kw_{1,2}f(x_{2,1}(t-\tau)) + pw_{3,4}f(x_{1,2}) \\ \dot{y}_{1,2} = c - dx_{1,2}^2 - y_{1,2} \\ \dot{z}_{1,2} = r(s(x_{1,2} + x_0) - z_{1,2}) \\ \dot{v}_{1,2} = -v_{1,2} + f(x_{2,1}(t-\tau)) \\ \dot{u}_{1,2} = -u_{1,2} + f(x_{1,2}) \end{cases} \quad (1)$$

其中, a, b, c, d, r, s, x_0 为系统参数, I 为外激励, $w_{1,2} = \alpha - \beta f(v_{1,2})$ 分别为神经元 1 和 2 间的连接强度, $w_{3,4} = \gamma - \varphi f(u_{1,2})$ 分别为神经元 1 和 2 上的连接强度, k 和 p 分别为耦合强度与自连接强度, τ 为耦合

2019-09-16 收到第 1 稿, 2019-11-25 收到修改稿.

* 国家自然科学基金资助项目(11872169 和 11472097), 江苏省自然科学基金资助项目(BK20191295), 河海大学中央高校基本科研业务费专项资金资助项目(2018B17514)

† 通讯作者 E-mail:maochen@hhu.edu.cn

时滞, f 为双曲正切函数.

若系统(1)存在平衡点 $E_0(x_{10}, y_{10}, z_{10}, v_{10}, u_{10}, x_{20}, y_{20}, z_{20}, v_{20}, u_{20})$, 引入坐标变换 $\bar{x}_i = x_i - x_{i0}$, $\bar{y}_i = y_i - y_{i0}$, $\bar{z}_i = z_i - z_{i0}$, $\bar{v}_i = v_i - v_{i0}$, $\bar{u}_i = u_i - u_{i0}$, 再将 $\bar{x}_i, \bar{y}_i, \bar{z}_i, \bar{v}_i, \bar{u}_i$ 分别改写为 x_i, y_i, z_i, v_i, u_i , 则有

$$\begin{cases} \dot{x}_{1,2} = y_{1,2} + y_{10,20} - a(x_{1,2} + x_{10,20})^3 + \\ \quad b(x_{1,2} + x_{10,20})^2 - z_{1,2} - z_{10,20} + I + \\ \quad k(\alpha - \beta f(v_{1,2} + v_{10,20})) \cdot \\ \quad f(x_{2,1}(t-\tau) + x_{20,10}) + p(\gamma - \\ \quad \varphi f(u_{1,2} + u_{10,20})) \cdot f(x_{1,2} + x_{10,20}) \\ \dot{y}_{1,2} = c - d(x_{1,2} + x_{10,20})^2 - y_{1,2} - y_{10,20} \\ \dot{z}_{1,2} = r(s(x_{1,2} + x_{10,20} + x_0) - z_{1,2} - z_{10,20}) \\ \dot{v}_{1,2} = -v_{1,2} - v_{10,20} + f(x_{2,1}(t-\tau) + x_{20,10}) \\ \dot{u}_{1,2} = -u_{1,2} - u_{10,20} + f(x_{1,2} + x_{10,20}) \end{cases} \quad (2)$$

对于对称平衡点 $E'_0(x_{10}, y_{10}, z_{10}, v_{10}, u_{10}, x_{10}, y_{10}, z_{10}, v_{10}, u_{10})$, 在其附近线性化系统的特征方程为

$$\Delta(\lambda, \tau) = \begin{vmatrix} \lambda I - A & -B \\ -B & \lambda I - A \end{vmatrix} = \Delta^+(\lambda, \tau) \cdot \Delta^-(\lambda, \tau) = \\ (P(\lambda) + Q(\lambda)e^{-\lambda\tau}) \cdot (P(\lambda) - Q(\lambda)e^{-\lambda\tau}) = 0 \quad (3)$$

其中, $P(\lambda) = ((\lambda + r)((\lambda + 1)(\lambda + h_1) + 2dx_{10} - h_3h_5) + (\lambda + 1)rs)(\lambda + 1)^2$, $Q(\lambda) = ((\lambda + 1)h_4 - h_2h_5)(\lambda + r)(\lambda + 1)^2$, $h_1 = 3ax_{10}^2 - 2bx_{10} - p(\gamma - \varphi f(u_{10}))(1 - f^2(x_{10}))$, $h_2 = k\beta f(x_{10})(1 - f^2(v_{10}))$, $h_3 = p\varphi f(x_{10})(1 - f^2(u_{10}))$, $h_4 = -k(\alpha - \beta f(v_{10}))(1 - f^2(x_{10}))$, $h_5 = f^2(x_{10}) - 1$,

$$A = \begin{bmatrix} -h_1 & 1 & -1 & -h_2 & -h_3 \\ -2dx_{10} & -1 & 0 & 0 & 0 \\ rs & 0 & -r & 0 & 0 \\ 0 & 0 & 0 & -1 & 0 \\ -h_5 & 0 & 0 & 0 & -1 \end{bmatrix},$$

$$B = \begin{bmatrix} h_4 e^{-\lambda\tau} & 0 & 0 & 0 & 0 \\ 0 & 0 & 0 & 0 & 0 \\ 0 & 0 & 0 & 0 & 0 \\ h_5 e^{-\lambda\tau} & 0 & 0 & 0 & 0 \\ 0 & 0 & 0 & 0 & 0 \end{bmatrix}.$$

为确定系统的稳定性, 假设 $\lambda = i\omega$ 为式(3)的一对纯虚根, 分离 $\Delta^\mp(i\omega, \tau) = 0$ 的实部和虚部可得:

$$\begin{cases} P_R(\omega) \mp Q_R(\omega) \cos(\omega\tau) \mp Q_I(\omega) \sin(\omega\tau) = 0 \\ P_I(\omega) \mp Q_I(\omega) \cos(\omega\tau) \pm Q_R(\omega) \sin(\omega\tau) = 0 \end{cases} \quad (4)$$

其中, $P_R(\omega) = l_1\omega^4 + l_2\omega^2 + l_3$, $P_I(\omega) = \omega^5 + l_4\omega^3 + l_5\omega$, $Q_R(\omega) = l_6\omega^4 + l_7\omega^2 + l_8$, $Q_I(\omega) = l_9\omega^3 + l_{10}\omega$, $l_1 = h_1 + r + 3$, $l_2 = -(2dx_{10} - h_3h_5)(r + 2) - 3(h_1(r + 1) + r(s + 1)) - 1$, $l_3 = 2dx_{10} - h_3h_5 + h_1r + rs$, $l_4 = -2dx_{10} - h_1r + h_3h_5 - rs - 3h_1 - 3r - 3$, $l_5 = (2dx_{10} - h_3h_5)(2r + 1) + 3r(h_1 + s) + h_1 + r$, $l_6 = h_4$, $l_7 = h_2h_5(r + 2) - 3h_4(r + 1)$, $l_8 = r(h_4 - h_2h_5)$, $l_9 = -h_4(r + 3) + h_2h_5$, $l_{10} = -h_2h_5(2r + 1) + h_4(3r + 1)$.

消去式(4)中的谐波项, 可得:

$$D^\mp(\omega) = \omega^{10} + g_1\omega^8 + g_2\omega^6 + g_3\omega^4 + g_4\omega^2 + g_5 = 0 \quad (5)$$

其中, $g_1 = l_1^2 - l_6^2 + 2l_4$, $g_2 = 2l_1l_2 + l_4^2 - 2l_6l_7 - l_9^2 + 2l_5$, $g_3 = 2l_1l_3 - 2l_{10}l_9 + l_2^2 + 2l_4l_5 - 2l_6l_8 - l_7^2$, $g_4 = -l_{10}^2 + 2l_2l_3 + l_5^2 - 2l_7l_8$, $g_5 = l_3^2 - l_8^2$. 若式(5)存在正实根 ω_i^\mp , 则相应的临界时滞为 $\tau_{i,j}^\mp = (\Phi_i^\mp + 2j\pi)/\omega_i^\mp$, $j = 0, 1, \dots, \Phi_i^\mp \in [0, 2\pi)$ 且满足

$$\begin{cases} \sin(\Phi_i^\mp) = \frac{\pm P_R(\omega_i^\mp) Q_I(\omega_i^\mp) \mp P_I(\omega_i^\mp) Q_R(\omega_i^\mp)}{Q_R^2(\omega_i^\mp) + Q_I^2(\omega_i^\mp)} \\ \cos(\Phi_i^\mp) = \frac{\pm P_R(\omega_i^\mp) Q_R(\omega_i^\mp) \pm P_I(\omega_i^\mp) Q_I(\omega_i^\mp)}{Q_R^2(\omega_i^\mp) + Q_I^2(\omega_i^\mp)} \end{cases} \quad (6)$$

根据时滞动力系统的稳定性和分叉理论^[14]可知: 若式(5)没有正实根, 则系统(1)平衡点的稳定性与时滞无关; 若存在正实根, 则系统可能发生有限次的稳定性切换, 且最终是不稳定的.

2 数值算例

(1) 系统参数取为 $a = 1, b = 3, c = 1, d = 5, s = 1, x_0 = 1.6, I = 1, r = 0.006, k = 0.8, \alpha = 1, \beta = 0.72, p = -0.8, \gamma = 1, \varphi = 0.6$. 经计算可知, 系统(1)存在对称平衡点 $E_0(0.252, 0.683, 1.852, 0.247, 0.247, 0.252, 0.683, 1.852, 0.247, 0.247)$. 本文主要分析此平衡点的局部稳定性. 当不含时滞时, 系统(1)存在正实部特征根, 则平衡点不稳定. 当存在时滞时, 求解式(5)可得 $\omega_1^\mp = 1.01$ 和 $\omega_2^\mp = 1.659$, 对应的临界时滞分别为 $\tau_{1,j}^- = 3.61, 9.86, \dots, \tau_{2,j}^- = 0.97, 4.76, \dots, \tau_{1,j}^+ = 0.49, 6.74, \dots, \tau_{2,j}^+ = 2.87, 6.65, \dots$. 随着时滞由零不断增大, 每当跨越临界时滞 $\tau_{1,j}^\mp$ 时, $\Delta^\mp(\lambda, \tau) = 0$

有一对特征根自右向左穿过虚轴;每当跨过临界时滞 $\tau_{2,0}^+$ 时, $\Delta^+(\lambda, \tau) = 0$ 有一对特征根自左向右穿过虚轴.因此,系统(1)在跨越临界时滞 $\tau_{1,0}^+$ 后处于稳定状态,而当跨过 $\tau_{2,0}^-$ 后平衡点失稳,并出现周期运动.综上可知,系统平衡点的稳定区域为 $(\tau_{1,0}^+, \tau_{2,0}^-)$, 不稳定区域为 $(0, \tau_{1,0}^+) \cup (\tau_{2,0}^-, +\infty)$.

如图1(a)所示,当 $\tau = 0.45$ 时,两神经元的运动趋于完全同步的周期振荡状态;图1(b)表示当 $\tau = 0.55$ 时,系统运动状态收敛到稳定的平衡点处;图1(c)表明当 $\tau = 1$ 时,平衡点失去稳定,两神经元出现异步周期振荡.上述现象表明:随着时滞的变化,系统经历了同步周期振荡、稳定平衡态以及异步周期振荡.

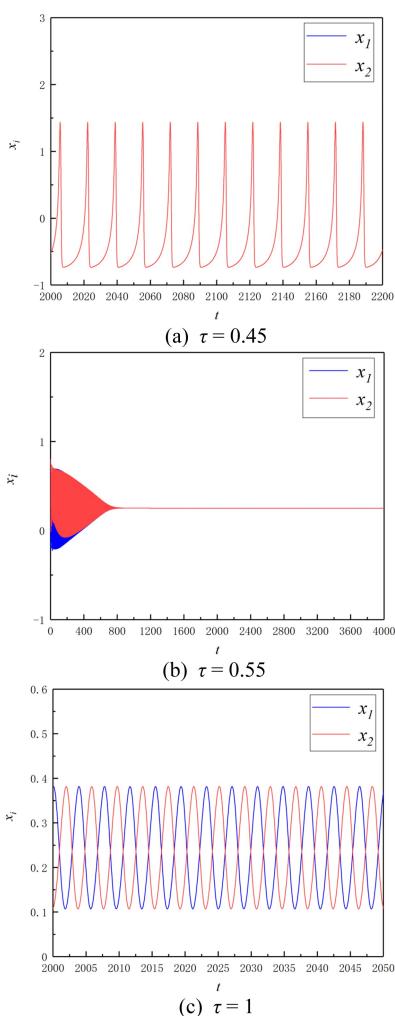
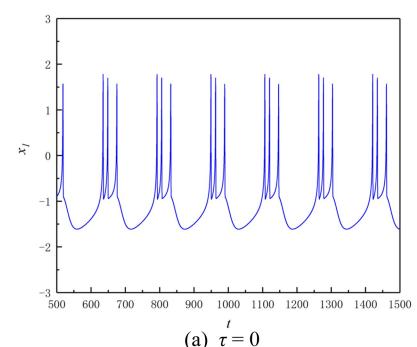


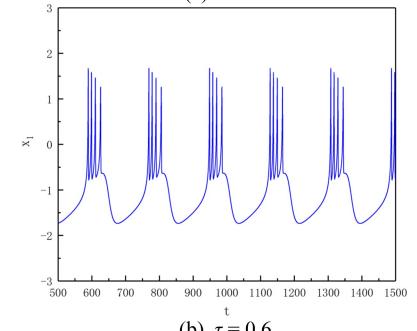
图1 系统(1)的响应

Fig.1 The responses of the system(1)

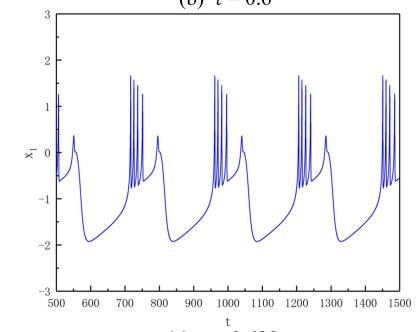
(2) 系统参数取为 $a=1, b=3, c=1, d=5, s=4, x_0=1.6, I=2, r=0.005, k=0.8, \alpha=1, \beta=0.72, p=-0.8, \gamma=1, \varphi=0.74$. 图2为系统(1)随时滞变化的响应.



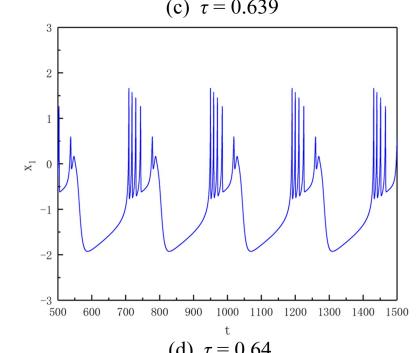
(a) $\tau = 0$



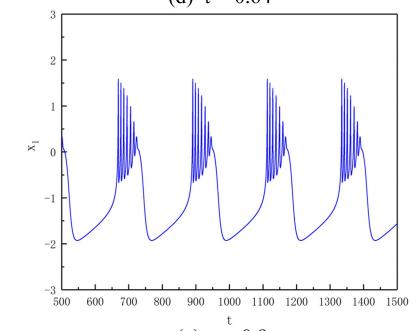
(b) $\tau = 0.6$



(c) $\tau = 0.639$



(d) $\tau = 0.64$



(e) $\tau = 0.9$

图2 系统(1)放电模式

Fig.2 Firing patterns of the system(1)

如图2(a)所示,无时滞时,神经元出现了周期3的簇放电行为;当 $\tau = 0.6$ 时,图2(b)表明神经元

簇放电中的峰增加了一个,产生了周期 4 的簇放电;随着时滞不断增加,如图 2(c)~(e)所示,簇放电中峰的个数由五逐步增加到七.图 2 表明神经元放电呈现加周期分叉的规律.

3 电路仿真

如图 3 所示, 电路仿真实验由 HR 神经元电

$$\left. \begin{aligned}
& R_{i,1} C_{i,1} \frac{dX_{1,2}}{dt'} = \frac{R_{i,4}}{R_{i,7}} Y_{1,2} - \frac{R_{i,4}}{R_{i,8}} X_{1,2}^3 + \frac{R_{i,4}}{R_{i,9}} X_{1,2}^2 - \frac{R_{i,4}}{R_{i,10}} Z_{1,2} + \frac{R_{i,12}}{R_{i,11} + R_{i,12}} \cdot \frac{R_{i,4}}{R_{i,13}} \cdot Vcc + \left(\frac{R_{i,4}}{R_{a1,2}} - \right. \\
& \left. \frac{0.1R_{i,4}}{R_{b1,2}} f(V_{1,2}) \right) f(X_{2,1}(t' - \tau')) + \left(\frac{R_{i,4}}{R_{a3,4}} - \frac{0.1R_{i,4}}{R_{b3,4}} f(U_{1,2}) \right) f(X_{1,2}) \\
& R_{i,2} C_{i,2} \frac{dY_{1,2}}{dt'} = \frac{R_{i,15}}{R_{i,14} + R_{i,15}} \cdot \frac{R_{i,5}}{R_{i,16}} \cdot Vcc - \frac{R_{i,5}}{R_{i,17}} Y_{1,2} - \frac{R_{i,5}}{R_{i,18}} X_{1,2}^2 \\
& R_{i,3} C_{i,3} \frac{dZ_{1,2}}{dt'} = \frac{R_{i,20}}{R_{i,19} + R_{i,20}} \cdot \frac{R_{i,6}}{R_{i,21}} \cdot Vcc - \frac{R_{i,6}}{R_{i,22}} Z_{1,2} + \frac{R_{i,6}}{R_{i,23}} X_{1,2} \\
& RC \frac{dV_{1,2}}{dt'} = -V_{1,2} + f(X_{2,1}(t' - \tau')) \\
& RC \frac{dU_{1,2}}{dt'} = -U_{1,2} + f(X_{1,2})
\end{aligned} \right\} (7)$$

其中, X_i, Y_i, Z_i, V_i, U_i 分别表示第 i 个神经元的输出电压. 显然, 式(1)为上述电路方程的无量纲形

路、时滞电路、忆阻器电路等组成.其中,HR 神经元电路由积分电路、加法电路以及乘法电路等组成;时滞模块 delay 由 RC 低通滤波器实现^[15];忆阻器模块 W_i 由-tanh 电路和乘法电路等模块构成^[15],而负双曲正切函数电路模块则由三极管、运算放大器以及电阻等器件构成.

图 3 所示的电路系统可用如下方程描述：

式,其参数与电路参数之间满足下列关系: $t=t'/R_{i,j}$
 $C_{i,j}, \tau=\tau'/R_{i,j}C_{i,j}$.

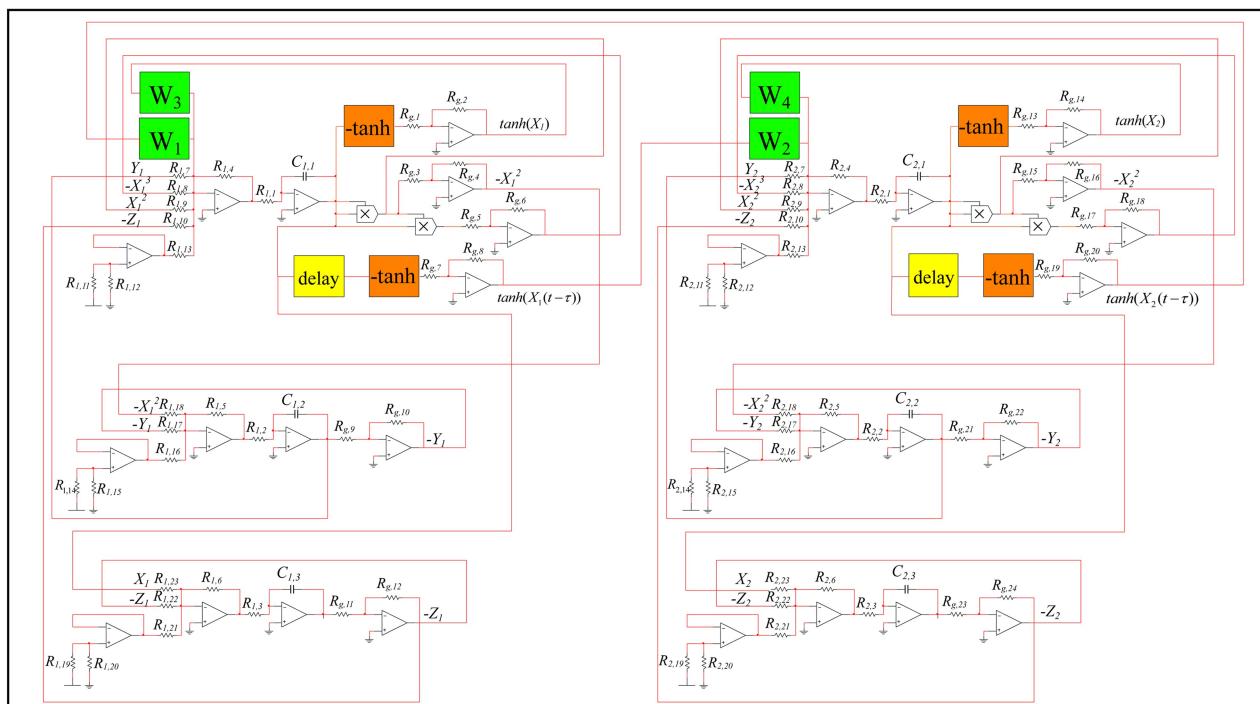


图 3 系统(7)电路原理图

Fig.3 A circuit implementation of the system(7)

(1) 电路参数为: $R_{i,1} = 1\text{K}\Omega$, $R_{i,2} = 1\text{K}\Omega$, $R_{i,3} = 1\text{K}\Omega$, $R_{i,4} = 10\text{K}\Omega$, $R_{i,5} = 10\text{K}\Omega$, $R_{i,6} = 1\text{K}\Omega$, $R_{i,7} =$

$$10\text{K}\Omega, R_{i,8} = 10\text{K}\Omega, R_{i,9} = 3.3\text{K}\Omega, R_{i,10} = 10\text{K}\Omega, R_{i,11} = 9\text{K}\Omega, R_{i,12} = 1\text{K}\Omega, R_{i,13} = 15\text{K}\Omega, R_{i,14} = 9\text{K}\Omega, R_{i,15} =$$

1K Ω , $R_{i,16} = 15K\Omega$, $R_{i,17} = 10K\Omega$, $R_{i,18} = 2K\Omega$, $R_{i,19} = 14.6K\Omega$, $R_{i,20} = 1K\Omega$, $R_{i,21} = 100K\Omega$, $R_{i,22} = 166.67K\Omega$, $R_{i,23} = 166.67K\Omega$, $R_{g,n} = 1K\Omega$, $C_{i,j} = 1\mu F$, $V_{cc} = 15V$, $i = 1, 2, j = 1, 2, 3, n = 1, 2, \dots, 24$. 忆阻器中电阻参数为 $R_{a1} = R_{a2} = 12.5K\Omega$, $R_{b1} = R_{b2} = 1.74K\Omega$, $R_{a3} = R_{a4} = 12.5K\Omega$, $R_{b3} = R_{b4} = 2.1K\Omega$, $R = 1K\Omega$, $C = 1\mu F$. 如图 4 所示, 电路 X_i 的输出电压经历同步周期振荡、直流电压、反相同步周期振荡. 图 5 为随着时滞变化, x_1 的振幅和频率的数值计算与电路仿真结果的对比图. 显然, 两者相吻合.

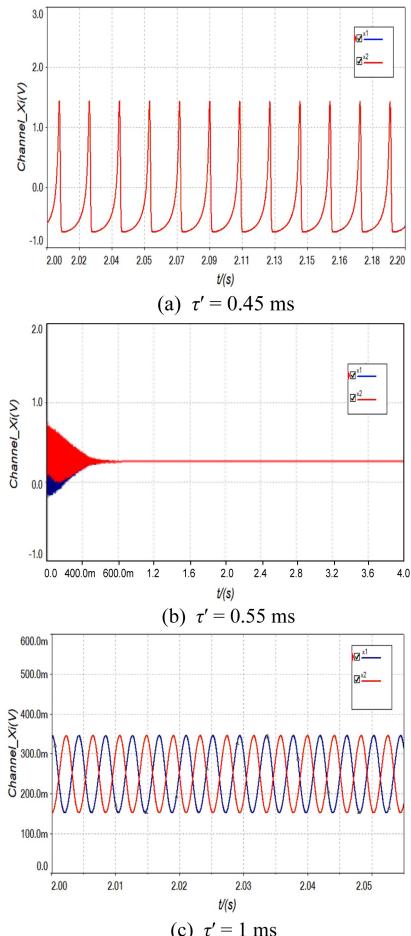


图4 系统(7) X_i 的输出电压

Fig.4 The output voltages X_i in the system (7)

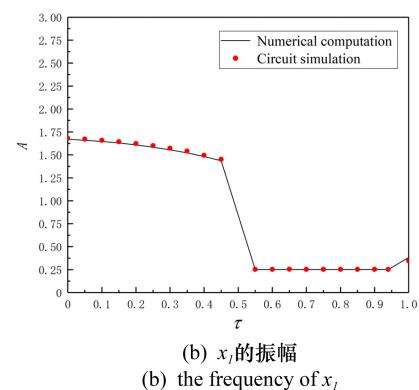
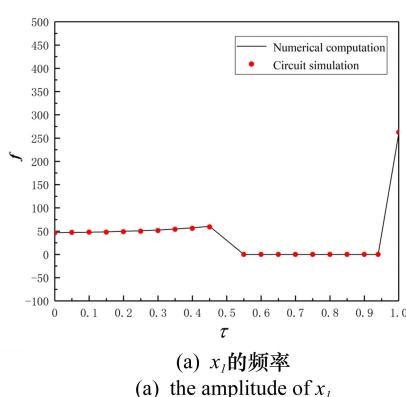
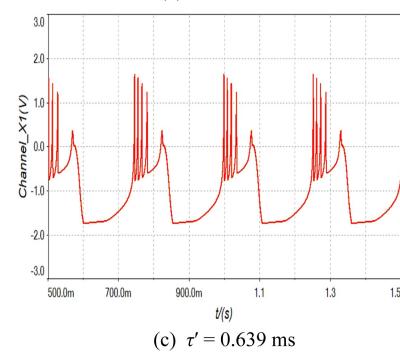
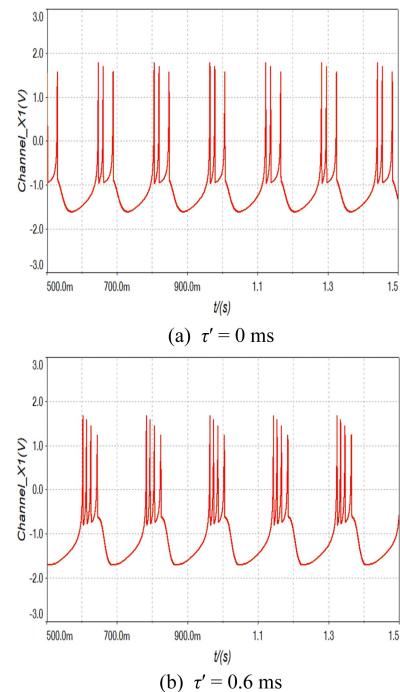


图 5 电路仿真与数值结果对比图

Fig.5 The results of circuit simulations and numerical computations

(2) 电路参数为 $R_{i,13} = 7.5\text{K}\Omega$, $R_{i,19} = 3.69\text{K}\Omega$, $R_{i,22} = 200\text{K}\Omega$, $R_{i,23} = 50\text{K}\Omega$, $R_{b3} = R_{b4} = 1.69\text{K}\Omega$, 其他参数不变. 如图 6 所示, 随着时滞的增加, 神经元 X_i 的簇放电模式经历了由周期 3 到周期 7 的转迁. 通过对比图 2 和图 6 可知, 电路仿真结果与数值计算相一致.



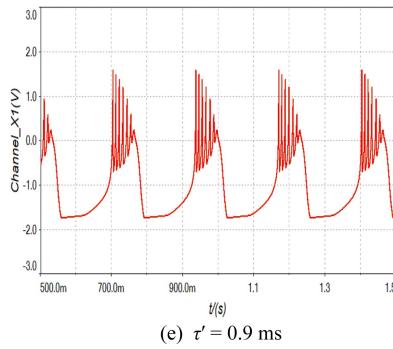
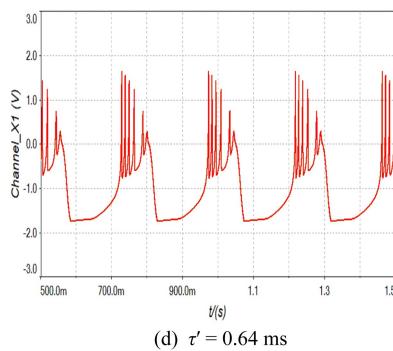


图6 电路系统(7)的放电模式

Fig.6 Firing patterns of the circuit system(7)

4 结论

本文研究了含时滞的忆阻耦合 HR 神经元系统.通过解耦与分析特征方程,讨论了平衡点的局部稳定性.借助数值算例验证了理论分析的结果,揭示了丰富的动力学现象.基于 HR 神经元电路、忆阻电路以及时滞电路等构建了电路实验平台,有效验证了已有结果.研究表明,时滞可诱导系统在稳定平衡态、同步周期振荡以及异步周期振荡之间发生切换.此外,时滞可诱导复杂放电模式的产生和相互间的转迁.例如,随着时滞的增大,神经元簇放电行为中峰的个数也不断增加,会经历由周期 3 至周期 7 的转迁过程.

参 考 文 献

- 1 Hodgkin A L, Huxley A F. A quantitative description of membrane current and its application to conduction and excitation in nerve. *The Journal of Physiology*, 1952, 117 (4): 500~544
- 2 Hindmarsh J L, Rose R M. A model of the neuronal bursting using three coupled first order differential equations. *Proceedings of the Royal Society B: Biological Sciences*, 1984, 221 (1222): 87~102

- 3 Wang H X, Wang Q Y, Lu Q S, et al. Equilibrium analysis and phase synchronization of two coupled HR neurons with gap junction. *Cognitive Neurodynamics*, 2013, 7 (2): 121~131
- 4 Ma J, Song X L, Jin W Y, et al. Autapse-induced synchronization in a coupled neuronal network. *Chaos, Solitons & Fractals*, 2015, 80: 31~38
- 5 茅晓晨.时滞耦合系统动力学的研究进展.动力学与控制学报,2017,15 (4): 295~306 (Mao X C. Advances in dynamics for coupled systems with time delays. *Journal of Dynamics and Control*, 2017, 15 (4): 295~306 (in Chinese))
- 6 Lakshmanan S, Lim C P, Nahavandi S, et al. Dynamical analysis of the Hindmarsh-Rose neuron with time delays. *IEEE Transactions on Neural Networks and Learning Systems*, 2016: 1~6
- 7 Steur E, Murguia C, Fey R H B, et al. Synchronization and partial synchronization experiments with networks of time-delay coupled Hindmarsh-Rose neurons. *International Journal of Bifurcation and Chaos*, 2016, 26 (7): 1650111. 1~20
- 8 曹淑红,段利霞,唐旭晖,等.具有时滞的耦合 Hindmarsh-Rose 神经元系统的放电模式.动力学与控制学报,2012,10(1): 88~91 (Cao S H, Duan L X, Tang X H, et al. Firing patterns in coupled Hindmarsh-Rose neural system with time-delay. *Journal of Dynamics and Control*, 2012, 10 (1): 88~91 (in Chinese))
- 9 Strukov D B, Snider G S, Stewart D R, et al. The missing memristor found. *Nature*, 2008, 453 (7191): 80~83
- 10 Chua L. Memristor-The missing circuit element. *IEEE Transactions on Circuit Theory*, 1971, 18 (5): 507~519
- 11 Bao B C, Qian H, Xu Q, et al. Coexisting behaviors of asymmetric attractors in Hyperbolic-Type memristor based hopfield neural network. *Frontiers in Computational Neuroscience*, 2017, 11: 81~95
- 12 Zhang J H, Liao X F. Effects of initial conditions on the synchronization of the coupled memristor neural circuits. *Nonlinear Dynamics*, 2019, 95 (2): 1269~1282
- 13 Thottil S K, Ignatius R P. Nonlinear feedback coupling in Hindmarsh-Rose neurons. *Nonlinear Dynamics*, 2016, 87 (3): 1~21
- 14 Hu H Y, Wang Z H. Dynamics of controlled mechanical systems with delayed feedback. Heidelberg: Springer-Verlag, 2002
- 15 乔磊,茅晓晨.时滞诱发的忆阻型 Hopfield 神经网络的复杂动力学.动力学与控制学报,2019,17(4):384~390 (Qiao L, Mao X C. Delay-induced complicated dynamics of a memristive Hopfield neural network. *Journal of Dynamics and Control*, 2019, 17 (4): 384~390 (in Chinese))

COMPLEX FIRING BEHAVIORS OF A MEMRISTIVE HR NEURONS WITH TIME DELAYS *

Wang Song Mao Xiaochen[†]

(College of Mechanics and Materials, Hohai University, Nanjing 211100, China)

Abstract In this paper, a two-coupled Hindmarsh-Rose neuronal system with memristors is studied and the effects of the transmission time delay between neurons are taken into account. By analyzing the stability of the equilibrium point, the delay-dependent stability conditions are obtained. Numerical simulations are performed to justify the theoretical results and a variety of rich and interesting dynamical phenomena are also explored, such as different firing behaviors. The platform of the circuit experiment for the coupled neurons is built and the revealed phenomena reach a good agreement with the obtained results. It is shown that the time delay plays important roles in the stability and firing behaviors of the system.

Key words Hindmarsh-Rose neuron, time delay, memristor, firing behavior, circuit experiment

Received 16 September 2019, Revised 25 November 2019.

* The project supported by the National Natural Science Foundation of China (11872169 and 11472097), Natural Science Foundation of Jiangsu Province (BK20191295) and Fundamental Research Funds for the Central Universities under Grant (2018B17514)

† Corresponding author E-mail: maochen@hhu.edu.cn